

**Femtosecond soft x-ray lasing in dense collisionally-pumped plasma**

Adeline Kabacinski , Fabien Tissandier, Julien Gautier, Jean-Philippe Goddet, Igor Andriyash, Philippe Zeitoun, and Stéphane Sebban\*

*Laboratoire d'Optique Appliquée, ENSTA-Paristech, CNRS, Ecole Polytechnique, Institut Polytechnique de Paris, 828 Bv des Maréchaux, 91762 Palaiseau, France*

Eduardo Oliva 

*Instituto de Fusión Nuclear “Guillermo Velarde” and Departamento de Ingeniería Energética, E.T.S.I. Industriales, Universidad Politécnica de Madrid, 28040 Madrid, Spain*

Michaela Kozlová 

*ELI Beamlines Project, Institute of Physics CAS, Praha 8, and Czech Republic Institute of Plasma Physics CAS, 182 00 Praha 8, Czech Republic*



(Received 4 April 2022; accepted 8 June 2022; published 18 July 2022)

We report the first experimental measurement of a strong pulse shortening of a seeded plasma-based soft x-ray laser at high electron densities. As a consequence of the gain gating caused by subsequent collisional ionization, the duration drops from 1.4 ps to an unprecedented value of 520 fs RMS when the electron density increases from 4 to  $7.6 \times 10^{19} \text{ cm}^{-3}$ . These measurements, performed with an original single-shot method, are in good agreement with results from 3D Maxwell-Bloch simulations.

DOI: [10.1103/PhysRevResearch.4.L032009](https://doi.org/10.1103/PhysRevResearch.4.L032009)

**Introduction.** Intense and short soft x-ray pulses offer possibilities for studying ultrafast phenomena in matter at the nanometer scale [1–3]. Collisional plasma-based soft x-ray lasers (SXRLs) have the advantage of producing high energy pulses [4] and being compact, therefore enabling, for instance, to perform holographic imaging, second harmonic generation for material science, and interferometry of high density plasmas [5–7]. A variety of SXRLs with energies ranging from 1  $\mu\text{J}$  to 10 mJ is now available in the wavelength range 6–63 nm [8–10] at a repetition rate up to 400 Hz [11].

However, the pulse duration of these sources is still rather long, ranging from 1.1 ps [12,13] up to 100 ps [4], thus limiting the scope of possible applications. To overcome this constraint, the transposition of chirped pulse amplification technique to the soft x-ray range has been proposed [14]. This theoretical scheme inferred SXRL pulses as short as 200 fs but to our knowledge has not been experimentally demonstrated so far. Other research directions have been considered to bring SXRL in the ultrafast domain. The so-called recombination scheme [15] in plasmas is an attractive candidate, but requires drastic plasma conditions. More recently, the innershell ionization scheme has demonstrated ultrafast durations in the

keV range, however this scheme requires a very intense hard x-ray free-electron laser [16].

Our work is based on an alternative approach relying on the collisional ionization gating of the gain media [17]. In the collisional pumping scheme, the population inversion allowing for a soft x-ray emission is achieved thanks to electron-ion collisions. When the plasma density is increased, more frequent collisions lead to higher gain and saturation intensity but also to an overionization of the lasing ion. It provokes a premature interruption of the gain, which should result in an expected shorter pulse duration. Observation of this feature was made possible by seeding the SXRL amplifier using a highorder harmonic (HH) source at the wavelength of the lasing transition. The gain duration of the seeded amplifier was measured [17] to be as short as 450 fs FWHM for an electron density of  $10^{20} \text{ cm}^{-3}$  by varying the timing of injection of the seed pulse into the amplifier. Although sub-picosecond duration pulses have been inferred at high densities by simulations, no direct measurement of the SXRL pulse duration had been performed so far in these extreme conditions.

This paper experimentally demonstrates a significant and systematic reduction of the seeded SXRL pulse duration when increasing the density of the amplifier. We measured an SXRL pulse duration as short as 520 fs RMS, therefore breaking the picosecond barrier and opening the path to much shorter durations at higher lasing densities. This investigation was made possible as a consequence of the development of an original jitterfree singleshot temporal profiler based on the rapid reflectivity drop of a soft x-ray multilayer mirror following its irradiation by an ultrashort infrared pulse. It is suited to soft x-ray pulses which are not intense enough to

\*stephane.sebban@ensta-paris.fr

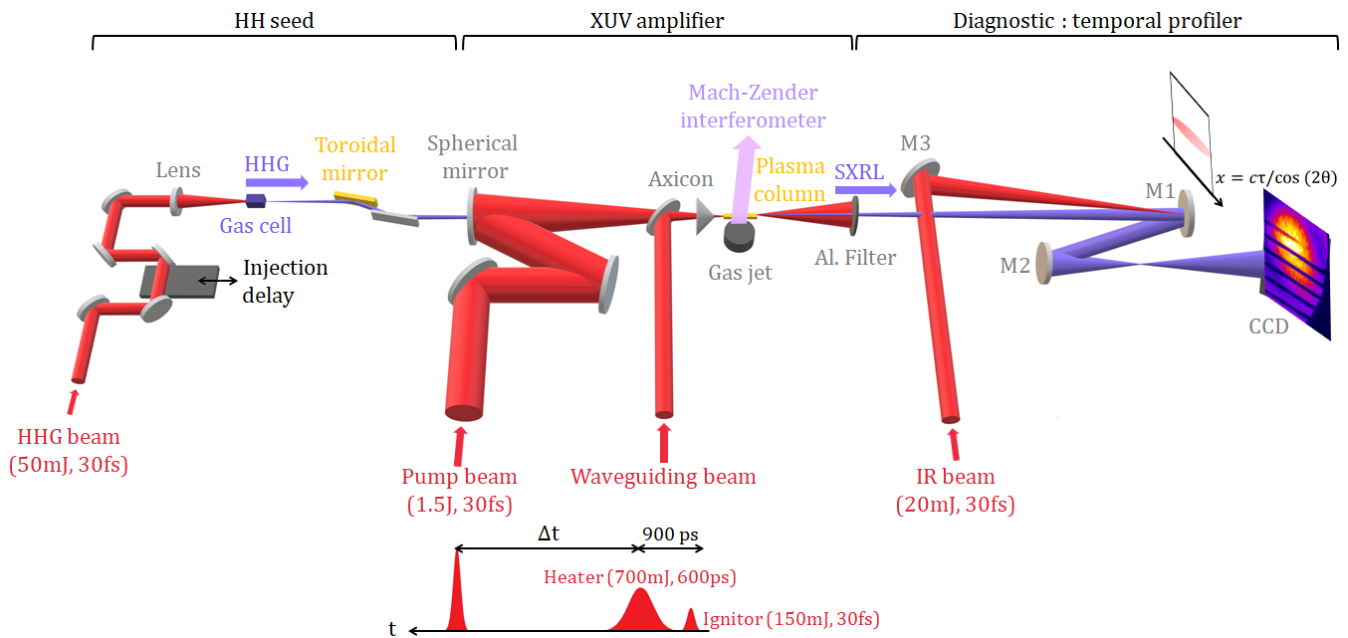


FIG. 1. Experimental setup: generation of the seeded soft x-ray laser and measurement of its temporal profile using a single-shot diagnostic. The soft x-ray beam arrives on a soft x-ray multilayer mirror (M1) with a near-normal incidence. The multilayer mirror is then imaged with a soft x-ray spherical mirror (M2) on a CCD camera. M1 is pumped in a traveling wave geometry by an infrared beam (20 mJ, 30 fs) using an oblique incidence spherical mirror (M3). An example of a measurement is shown, representing the recorded image of the partially reflected SXRL beam on the damaged multilayer mirror. The line on the top corresponds to the current shot, for which the infrared laser is currently propagating. Those on the bottom are post-mortem shots for which the infrared line has already traveled.

induce ultrafast changes of optical properties in matter, and is useful to measure the envelope of their temporal profile even if asymmetric with a femtosecond resolution. Moreover, this method can achieve a measurement in a singleshot where most of the other existing techniques require the previous knowledge of reference measurements.

**Experimental Setup.** The experiment was performed at Laboratoire d’Optique Appliquée using a multi-terawatt Ti:Sa laser system providing several beams at 1 Hz around a central wavelength of 820 nm. A first pulse of 1.5 J and 30 fs was focused into a 10 mm long gas jet of krypton, resulting in an intensity of  $4 \times 10^{18} \text{ Wcm}^{-2}$ , to generate a Ni-like Kr soft x-ray amplifier emitting at a wavelength of 32.8 nm (Fig. 1) [18].

To overcome the strong refraction preventing the pump beam propagation along the full length of the gas jet, a second beam was used to preform a plasma waveguide. The beam was composed of two pulses: an “igniter” pulse (150 mJ, 30 fs) followed 900 ps later by a “heater” pulse (700 mJ, 600 ps), both focused by an axicon lens over the whole gas length [19]. The electron density builds up as first electrons generated by the “igniter” get heated and foster avalanche collisional ionization. After 1 ns, the natural hydrodynamic plasma expansion provokes a consequent ejection of electrons. The plasma channel then spreads out, and the density gradient decreases with time [20]. By adjusting the delay  $\Delta t$  between the waveguiding sequence and the pump beam, the amplifier electron density can thus be varied in the range from 4 to  $7.6 \times 10^{19} \text{ cm}^{-3}$ . The electron density was measured shot-to-shot using a Mach-Zender interferometer with an uncertainty of  $10^{19} \text{ cm}^{-3}$  [20].

To boost the SXRL output and improve its spatial quality [21,22], a “seed” HH pulse was generated using another

infrared pulse (30 mJ, 30 fs) focused in an argon-filled cell. The 25th harmonic signal was optimized by changing the gas pressure, the beam energy and the focusing conditions, and spectrally tuned onto the amplifier ASE laser line at 32.8 nm by chirping the HH driver beam. The output of the HH source was imaged at the entrance of the amplifying krypton plasma, using a grazing incidence gold coated toroidal mirror, allowing an efficient coupling into the SXRL gain region. The amplification of the seed by the krypton amplifier results in a 32.8 nm Gaussian-like beam profile with a divergence of about 1 mrad. The shot-to-shot pointing variations were estimated to be around 0.1 mrad RMS. In the best conditions, the output energy of our seeded 32.8 nm laser has been measured to be up to  $2 \mu\text{J}$  per shot.

To measure the SXRL pulse duration we have developed a new diagnostic enabling single-shot operation with a reasonable time resolution in the soft x-ray range. Existing temporal diagnostics such as streak cameras, cross-correlation techniques [23–25] or methods based on the laser-assisted photoelectric effect [26–28], on the inner-shell resonant absorption [29–31], or on the transient change of optical reflectivity [32] are very powerful tools. However, most of these techniques require several shots or the previous knowledge of reference measurements and are not able to simultaneously provide sufficient temporal resolution and discriminate the front from the rear of the soft x-ray pulse, which is of importance in the case of SXRL where asymmetric gain temporal evolution is theoretically expected.

Our single-shot temporal profiler diagnostic is illustrated in Fig. 1. It is based on a pump-probe technique allowing measurement of the transient reflectivity of a laser-damaged soft x-ray mirror using the 32.8 nm laser as a probe. The

32.8 nm SXRL beam is reflected by a near-normal incidence B<sub>4</sub>C/Si multilayer mirror (M1) having 25% peak reflectivity. The M1 mirror surface is imaged onto a CCD camera using an  $f = 500$  mm soft x-ray spherical mirror (M2) with a magnification of 2. The 32.8 nm SXRL beam is used here to probe shot to shot the M1 mirror reflectivity. Simultaneously, an infrared pump beam (20 mJ, 30 fs), issued from the same laser system, ensuring an entirely jitter-free measurement, is focused on the M1 mirror surface using an  $f = 300$  mm spherical mirror (M3) at an incidence angle  $\theta$  comprised between  $30^\circ$  and  $38^\circ$  depending on the measurement (Fig. 1). The resulting 8-mm-long focus line deposits its energy on the mirror, ablating the mirror surface within a few tens of femtoseconds [33]. The laser intensity necessary to ensure a total extinction of the soft x-ray reflectivity was found to be lower than  $10^{14}$  Wcm<sup>-2</sup>. Aluminum foils, positioned just after the gas jet and in front of the CCD, are used to filter out the IR-coming from, respectively, the beam pumping the plasma amplifier and the beam pumping the multilayer mirror- from the x-ray signal.

This technique intrinsically causes the pump beam wavefront to be tilted with respect to the mirror surface, allowing the energy deposition on the mirror to travel along the focal line [34,35]. The corresponding spatial coordinate  $x$  in the multilayer mirror plane thus corresponds to  $\tau = x \cos(2\theta)/c$ , the arrival time of the infrared beam. The traveling wave velocity is therefore given by  $c/\cos(2\theta)$ , here comprised between  $2c$  and  $4c$ . The accurate synchronization of the pump pulse, as well as the calibration between spatial and temporal coordinates, were determined by scanning the infrared beam delay line. Since the multilayer mirror is reflective before pump energy deposition and absorbing when damaged, the reflected soft x-ray intensity profile arriving simultaneously with the infrared line, named  $I(x)$ , results from an integration of the temporal profile of the soft x-ray pulse:

$$I\left(x = \frac{c\tau}{\cos(2\theta)}\right) = I_0(x) \int_{-\infty}^{+\infty} \phi(t)R(t - \tau) dt \quad (1)$$

where  $\phi$  is the temporal intensity profile of the soft x-ray pulse,  $I_0$  represents the reference (i.e. reflected by undamaged mirror) spatial profile of the SXRL beam, and  $R$  is a Heaviside function equal to 1 if  $t - \tau < 0$  and 0 otherwise. This equation is similar to the one used when performing a knife-edge beam profile measurement [36]. It should be noted that, in this setup, the temporal window that can effectively be probed during the shot is given by the spatial extension of the soft x-ray line focus along the  $x$  direction. Here, this time span is about 4 ps which is sufficient considering the expected pulse duration.

Figure 2(a) shows the recorded image of the partially reflected SXRL beam on the damaged multilayer mirror at an electron density of  $7.6 \times 10^{19}$  cm<sup>-3</sup>. The line on the top represents the current shot, for which the infrared laser is currently propagating. The lines on the bottom are post-mortem shots for which the infrared laser has already traveled. The beam horizontal cross-sections  $I_0$  and  $I$ , plotted respectively in green and blue in Fig. 2(b), are extracted on a singleshot and fitted to avoid spurious numerical amplification of the noise during postprocessing. The reference intensity  $I_0$  has a Gaussian

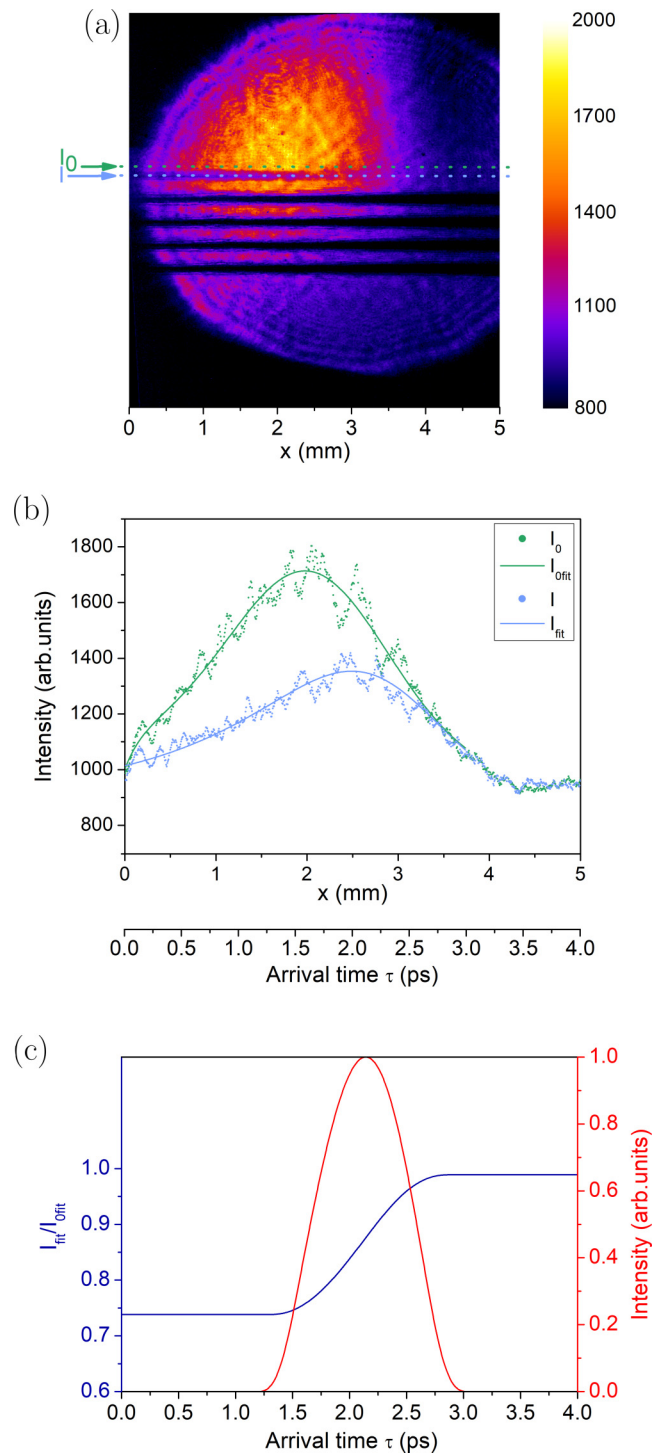


FIG. 2. Example of a single-shot reconstruction of the SXRL temporal profile at an electron density of  $7.6 \times 10^{19}$  cm<sup>-3</sup>:  $I_0$  and  $I$ , respectively in green and light blue, are recorded on a singleshot and are then fitted. The temporal profile in red is finally derived from the derivative of the ratio  $I_{fit}/I_{0fit}$  in dark blue.

shape. The intensity  $I$  is fitted with an exponentially modified Gaussian curve to conserve the reference shape while taking into account the ablating process. The normalized intensity profile is finally obtained by reversing the equation 1, i.e. by calculating the derivative of the ratio  $I_{fit}/I_{0fit}$ . This ratio,

as well as the reconstructed temporal profile, are plotted in Fig. 2(c). Since  $\tau$  represents the arrival time of the infrared beam, the origin of the temporal profile is arbitrary.

The resolution of the pulse duration measurement depends on a few factors: the multilayer mirror ablation time (about 30 fs), the uncertainty of the calibration between the spatial and the temporal coordinates (here 0.5 fs/pixel), the spatial resolution of the imaging system in the x direction (estimated to be around 50  $\mu\text{m}$  equivalent to 40 fs), and the fitting uncertainty which can induce a maximum error of 50 fs. The effective resolution of our diagnostic has been estimated to be as short as 200 fs.

**Results and discussion.** The purpose of this paper is to demonstrate experimentally the reduction of the SXRL pulse duration induced by the gain quenching at high densities down to the femtosecond time scale. An estimation of the gain duration can be obtained by measuring the soft x-ray intensity as a function of the delay between the creation of the plasma amplifier and the injection time of the HH seed. Figures 3(a) and 3(b) display this measurement in red for the respective electron densities of 4.4 and  $7.6 \times 10^{19} \text{ cm}^{-3}$ . Uncertainties are determined by measuring the repeatability over five shots. These data clearly show a stronger amplification of the seed pulse when the injection time is synchronized with the gain period and reveal the actual amplification dynamics at a given electron density. The amplification period is shorter and starts earlier with steeper slope for higher plasma densities. Here we inferred that the maximum amplification is respectively achieved at 1.8 ps and 1.2 ps after the plasma creation when electron density ranges from 4.4 to  $7.6 \times 10^{19} \text{ cm}^{-3}$ . The amplification respectively lasts for about 1.7 ps to 1.0 ps RMS. Indeed, collisional overionization of the lasing-ion is favored at high densities. As the amplifier lifetime strongly depends on the depletion rate of the lasing population, increasing the electron density results in a premature interruption of the lasing action. As a consequence, the amplification duration is shortened at high densities.

Jointly with the amplification dynamics, duration measurements of the 32.8 nm seeded SXRL have been performed for several electron densities. These measurements have been performed thanks to the above-described diagnostic. Reconstruction of the temporal profiles obtained for 4.4 and  $7.6 \times 10^{19} \text{ cm}^{-3}$  are respectively shown in green in Figs. 3(a) and 3(b). Here, the rising edge of the pulse is artificially set on the rising edge of the amplification dynamics. The RMS pulse duration has been measured to drop from  $1.2 \pm 0.3 \text{ ps}$  at  $4.4 \times 10^{19} \text{ cm}^{-3}$  to  $520 \pm 200 \text{ fs}$  at  $7.6 \times 10^{19} \text{ cm}^{-3}$ , which is the first direct measurement of a sub-picosecond SXRL pulse. The measured temporal profile shown in Fig. 3(b) is the shortest pulse obtained at this electron density. Furthermore, these measurements show that the temporal profile of the 32.8 nm SXRL exhibits the same faster rising edge at high densities as the measured amplification dynamics. It can be noted that the pulse duration is shorter than the amplification duration. This can be explained by the fact that the amplification duration is estimated by the measurement of the SXRL signal with respect to the harmonic injection delay. Since the SXRL signal is integrated over propagation and as the pump and seed pulses have inherently different group velocities, the measured amplification dynamics is longer than the theoretic

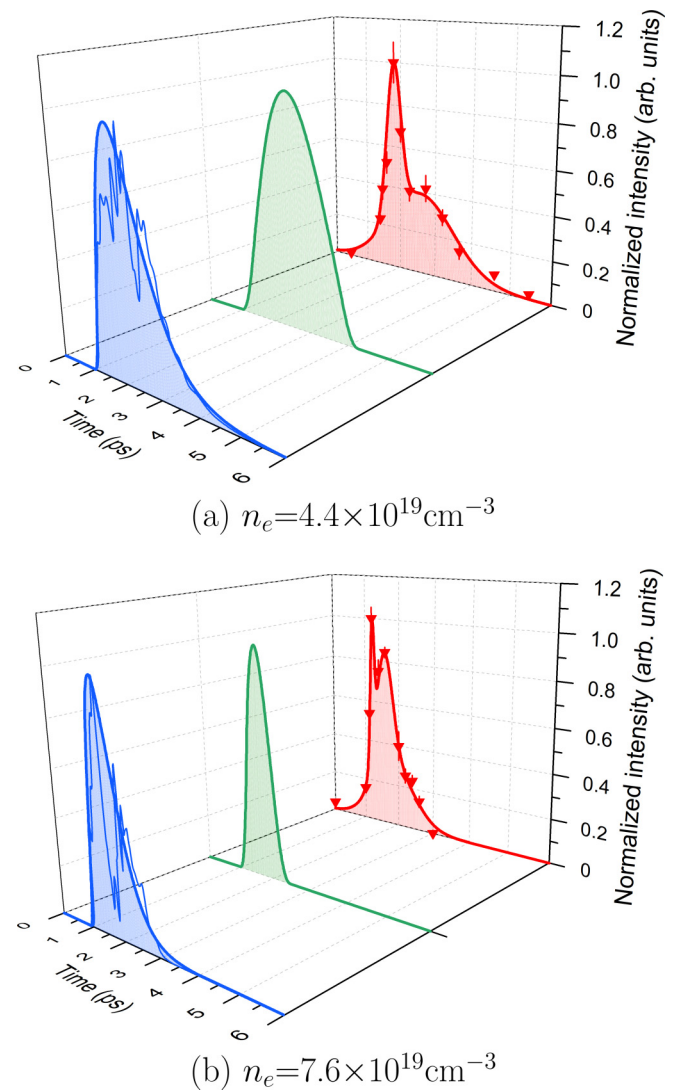


FIG. 3. Measured amplification dynamics in red, measured temporal profiles in green, and simulated temporal profiles in blue for different electron densities of the plasma amplifier. The measured temporal profile shown in the case of  $n_e = 7.6 \times 10^{19} \text{ cm}^{-3}$  is the shortest pulse obtained at this electron density.

cal gain duration and therefore longer than the pulse duration. Also it can be noticed that the SXRL pulse duration is much longer than the harmonics duration, which is due to the strong spectral gain narrowing induced by amplification [37].

Experimental temporal profiles have also been compared to simulated profiles obtained with the DAGON 3D Maxwell-Bloch code [38,39] which models the full spatio-temporal structure of the HH seed amplified through the plasma amplifier. DAGON uses as input the 3D structure of the plasma amplifier, as given by hydrodynamic and Particle-In-Cell (PIC) simulations. The creation and evolution of the plasma waveguide is modeled with the 2D radiative hydrodynamics code ARWEN [40,41]. This code solves the equations of compressible fluid dynamics coupled to energy transfer processes: electronic diffusion, radiative transfer, and laser propagation and absorption. The resulting density profile is fed to a 2D axisymmetric PIC code, FBPIC [42]. This code solves

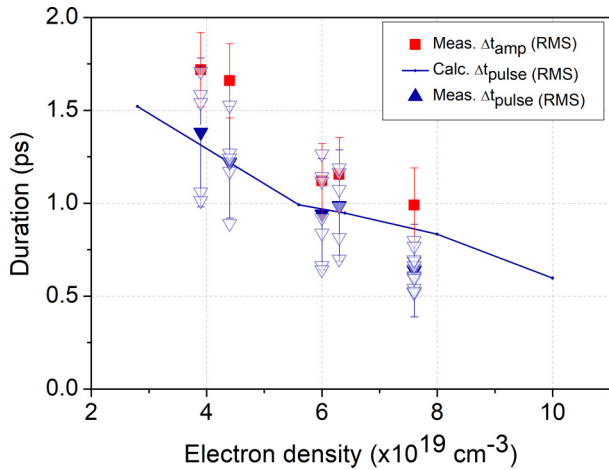


FIG. 4. Respectively in red and blue, RMS measured amplification duration ( $\Delta t_{\text{amp}}$ ) and RMS pulse duration ( $\Delta t_{\text{pulse}}$ ) with respect to the electron density of the plasma amplifier. Triangles and squares are used for measurements points. Filled symbols are used for averaging over few shots. Empty triangles stand for shot-to-shot measurements. Solid lines correspond to the 3D Maxwell-Bloch simulations.

Maxwell's equations and the relativistic motion equations for the macroparticles that model the plasma. The temporal dynamics of the lasing ion and population inversion is modeled with the collisional-radiative code OFIKinRad [43]. Nonequilibrium effects are taken into account by solving a Fokker-Planck equation to compute the electron energy distribution function and, afterwards, the cross sections. The output of FBIC and OFIKinRad is used by DAGON to compute the temporal dynamics of the plasma amplifier. DAGON solves the set of 3D Maxwell-Bloch equations in the paraxial and slowly varying envelope approximation, taking into account the temporal dynamics of the amplifier medium. The three-dimensional aspect of the code is required to take into account the plasma inhomogeneities [44], as well as the 3D stochastic structure of the Amplified Spontaneous Emission (ASE). We modeled a  $100 \mu\text{m} \times 100 \mu\text{m} \times 10 \text{mm}$  amplifier, using a mesh consisting in  $100 \times 100 \times 2000$  cells. The timestep was fixed to 10 fs. Simulations, shown in blue in Fig. 3, exhibit intensity modulations that can not be observed experimentally. The envelope of the simulated profiles is plotted on the same graph to ease the comparison with our measurements. When increasing the electron density from Fig. 3(a) to 3(b), the simulated RMS duration of the envelope is reduced from 1.5 ps to 0.8 ps, in good agreement with measurements. It can be noted that the simulated temporal profile has slightly faster rising time than falling edge in agreement with the shape observed in the temporal profile and amplification dynamics measurements.

Systematic measurements and simulations for electron densities ranging from  $3.9 \times 10^{19} \text{cm}^{-3}$  to  $10^{20} \text{cm}^{-3}$  have been performed. The corresponding RMS amplification and pulse durations are represented in Fig. 4. Squares and triangles stand for measurements, empty triangles are used for shot-to-shot measurements. The uncertainty on each pulse duration measurement point is obtained by taking into consideration the measurement uncertainty described above and the

repeatability uncertainty over between 5 and 10 shots, resulting in a total enlarged uncertainty on the RMS pulse duration comprised between 250 fs (for the highest densities) and 400 fs (for the lowest densities) depending on the measurement point. Measurements exhibit a monotonic reduction of the amplification duration from  $1.7 \pm 0.2 \text{ps}$  to  $1.0 \pm 0.2 \text{ps}$  RMS when the electron density is increased from  $3.9$  to  $7.6 \times 10^{19} \text{cm}^{-3}$ . The pulse duration appears to be strongly correlated to the amplification duration and is consequently reduced from  $1.4 \pm 0.4 \text{ps}$  down to  $640 \pm 250 \text{fs}$  RMS. The direct experimental demonstration of the pulse duration reduction induced by the gain quenching at high densities is therefore achieved for the first time. The shortest pulse duration that we obtained on a singleshot at  $7.6 \times 10^{19} \text{cm}^{-3}$  is  $520 \pm 200 \text{fs}$  RMS is the shortest collisional SXRL duration ever directly reported. The SXRL pulse duration values issued from the 3D Maxwell-Bloch calculations are plotted in solid lines on the same graph. Simulations are in good agreement with those experimental results, and predict that the pulse duration continues to decrease for density as high as  $10^{20} \text{cm}^{-3}$ , which is accessible although the current configuration does not allow to reach it.

*Conclusion.* In summary, we have demonstrated experimentally a femtosecond collisional plasma-based SXRL, with the first direct measurement of sub-picosecond pulses. Measurements exhibit a reliable decrease of the pulse duration, correlated with the reduction of the amplification period when the density increases up to  $7.6 \times 10^{19} \text{cm}^{-3}$ . An unprecedented duration of 520 fs has therefore been measured in close agreement with the theoretical predictions, thus experimentally breaking the decade-long picosecond range. The proposed original single-shot method is enabling to measure pulse duration for most fast and ultrafast sources in the soft x-ray range with a resolution as short as 200 fs. The simultaneous measurement of the unperturbed reference beam here is an asset in mitigating shot-to-shot fluctuations of the laser plasma-based soft x-ray sources. The measured temporal profiles are in agreement with 3D time-dependent Maxwell-Bloch simulations over a wide range of electron density therefore enabling the validation of plasma kinetic codes on a subpicosecond time scale. Simulations predict even shorter durations at  $10^{20} \text{cm}^{-3}$ , paving the way for numerous applications requiring high intensity soft x-ray pulses to excite or probe ultrafast processes in matter at nanometer scale.

*Acknowledgments.* This work is supported ‘‘Investissements d’Avenir’’ by Labex PALM (ANR-10-LABX-0039-PALM) and has received funding from the European Union’s Horizon 2020 research and innovation program under Grant Agreement No. 654148 Laserlab-Europe, and was also supported by Grant agency of the Czech Republic, Project No. 18-27340S. The authors acknowledge support from COST (European Cooperation in Science and Technology for funding the Action TUMIEE (CA17126) supporting this work. E.O. received funds from the Universidad Politecnica de Madrid and the Comunidad Autonoma de Madrid, linea de actuacion estimulo a la investigacion de jovenes doctores, project CROM and the Spanish Ministerio de Ciencia e Innovacion through a Ramon y Cajal RYC2018-026238-I fellowship.

- [1] K. Sokolowski-Tinten, C. Blome, J. Blums, A. Cavalleri, C. Dietrich, A. Tarasevitch, I. Uschmann, E. Förster, M. Kammler, M. H. von Hoegen, and D. von der Linde, Femtosecond X-ray measurement of coherent lattice vibrations near the Lindemann stability limit, *Nature (London)* **422**, 287 (2003).
- [2] E. Gagnon, P. Ranitovic, X.-M. Tong, C. L. Cocke, M. M. Murnane, H. C. Kapteyn, and A. S. Sandhu, Soft X-ray-driven femtosecond molecular dynamics, *Science* **317**, 1374 (2007).
- [3] H. N. Chapman, S. P. Hau-Riege, M. J. Bogan, S. Bajt, A. Barty, S. Boutet, S. Marchesini, M. Frank, B. W. Woods, W. H. Benner, R. A. London, U. Rohner, A. Szöke, E. Spiller, T. Möller, C. Bostedt, D. A. Shapiro, M. Kuhlmann, R. Treusch, E. Plönjes *et al.*, Femtosecond time-delay X-ray holography, *Nature (London)* **448**, 676 (2007).
- [4] B. Rus, T. Mocek, A. R. Präg, M. Kozlová, G. Jamelot, A. Carillon, D. Ros, D. Joyeux, and D. Phalippou, Multimillijoule, highly coherent X-ray laser at 21 nm operating in deep saturation through double-pass amplification, *Phys. Rev. A* **66**, 063806 (2002).
- [5] P. W. Wachulak, M. C. Marconi, R. A. Bartels, C. S. Menoni, and J. J. Rocca, Soft X-ray laser holography with wavelength resolution, *J. Opt. Soc. Am. B: Opt. Phys.* **25**, 1811 (2008).
- [6] T. Helk, E. Berger, S. Jamnuch, L. Hoffmann, A. Kabacinski, J. Gautier, F. Tissandier, J.-P. Goddet, H.-T. Chang, J. Oh, C. D. Pemmaraju, T. A. Pascal, S. Sebban, C. Spielmann, and M. Zuerch, Table-top extreme ultraviolet second harmonic generation, *Sci. Adv.* **7**, eabe2265 (2021).
- [7] J. Filevich, J. J. Rocca, E. Jankowska, E. C. Hammarsten, K. Kanizay, M. C. Marconi, S. J. Moon, and V. N. Shlyaptsev, Two-dimensional effects in laser-created plasmas measured with soft X-ray laser interferometry, *Phys. Rev. E* **67**, 056409 (2003).
- [8] A. Rockwood, Y. Wang, S. Wang, M. Berrill, V. N. Shlyaptsev, and J. J. Rocca, Compact gain-saturated X-ray lasers down to 6.85 nm and amplification down to 5.85 nm, *Optica* **5**, 257 (2018).
- [9] B. E. Lemoff, C. P. Barty, and S. E. Harris, Femtosecond-pulse-driven, electron-excited XUV lasers in eight-times-ionized noble gases, *Opt. Lett.* **19**, 569 (1994).
- [10] F. Tissandier, J. Gautier, J.-P. Goddet, A. Kabacinski, S. Sebban, J. Nejdil, M. Kozlová, and G. Maynard, Two-Color Soft X-Ray Lasing in a High-Density Nickel-like Krypton Plasma, *Phys. Rev. Lett.* **124**, 133902 (2020).
- [11] J. J. Rocca, B. A. Reagan, C. Baumgarten, Y. Wang, S. Wang, M. Pedicone, M. Berrill, V. N. Shlyaptsev, C. N. Kyaw, L. Yin, H. Wang, M. C. Marconi, and C. S. Menoni, Progress in high repetition rate soft X-ray laser development and pump lasers at Colorado State University, *X-ray Lasers and Coherent X-ray Sources: Development and Applications*, Vol. 10243 (SPIE, USA, 2017).
- [12] Y. Wang, M. Berrill, F. Pedaci, M. M. Shakya, S. Gilbertson, Z. Chang, E. Granados, B. M. Luther, M. A. Larotonda, and J. J. Rocca, Measurement of 1-ps soft X-ray laser pulses from an injection-seeded plasma amplifier, *Phys. Rev. A* **79**, 023810 (2009).
- [13] A. Klisnick, J. Kuba, D. Ros, R. Smith, G. Jamelot, C. Chenais-Popovics, R. Keenan, S. J. Topping, C. L. S. Lewis, F. Strati, G. J. Tallents, D. Neely, R. Clarke, J. Collier, A. G. MacPhee, F. Bortolotto, P. V. Nickles, and K. A. Janulewicz, Demonstration of a 2-ps transient X-ray laser, *Phys. Rev. A* **65**, 033810 (2002).
- [14] E. Oliva, M. Fajardo, L. Li, M. Pittman, T. T. T. Le, J. Gautier, G. Lambert, P. Velarde, D. Ros, S. Sebban, and P. Zeitoun, A proposal for multi-tens of GW fully coherent femtosecond soft X-ray lasers, *Nat. Photonics* **6**, 764 (2012).
- [15] P. Amendt, D. C. Eder, and S. C. Wilks, X-Ray Lasing by Optical-Field-Induced Ionization, *Phys. Rev. Lett.* **66**, 2589 (1991).
- [16] H. C. Kapteyn, Photoionization-pumped X-ray lasers using ultrashort-pulse excitation, *Appl. Opt.* **31**, 4931 (1992).
- [17] A. Depresseux, E. Oliva, J. Gautier, F. Tissandier, J. Nejdil, M. Kozlová, G. Maynard, J. P. Goddet, A. Tafzi, A. Lifschitz, H. T. Kim, S. Jacquemot, V. Malka, K. T. Phuoc, C. Thauray, P. Rousseau, G. Iaquaniello, T. Lefrou, A. Flacco, B. Vodungbo *et al.*, Table-top femtosecond soft X-ray laser by collisional ionization gating, *Nat. Photonics* **9**, 817 (2015).
- [18] S. Sebban, T. Mocek, D. Ros, L. Upcraft, P. Balcou, R. Haroutunian, G. Grillon, B. Rus, A. Klisnick, A. Carillon, G. Jamelot, C. Valentin, A. Rouse, J. P. Rousseau, L. Notebaert, M. Pittman, and D. Hulin, Demonstration of a Ni-Like Kr Optical-Field-Ionization Collisional Soft X-Ray Laser at 32.8 nm, *Phys. Rev. Lett.* **89**, 253901 (2002).
- [19] M. C. Chou, P. H. Lin, C. A. Lin, J. Y. Lin, J. Wang, and S. Y. Chen, Dramatic Enhancement of Optical-Field-Ionization Collisional-Excitation X-Ray Lasing by an Optically Preformed Plasma Waveguide, *Phys. Rev. Lett.* **99**, 063904 (2007).
- [20] E. Oliva, A. Depresseux, M. Cotel, A. Lifschitz, F. Tissandier, J. Gautier, G. Maynard, P. Velarde, and S. Sebban, Hydrodynamic evolution of plasma waveguides for soft X-ray amplifiers, *Phys. Rev. E* **97**, 023203 (2018).
- [21] P. Zeitoun, G. Faivre, S. Sebban, T. Mocek, A. Hallou, M. Fajardo, D. Aubert, P. Balcou, F. Burgy, D. Douillet, S. Kazamias, G. de Lachèze-Murel, T. Lefrou, S. le Pape, P. Mercère, H. Merdji, A. S. Morlens, J. P. Rousseau, and C. Valentin, A high-intensity highly coherent soft X-ray femtosecond laser seeded by a high harmonic beam, *Nature (London)* **431**, 426 (2004).
- [22] Y. Wang, E. Granados, F. Pedaci, D. Alessi, B. Luther, M. Berrill, and J. J. Rocca, Phase-coherent, injection-seeded, table-top soft X-ray lasers at 18.9 nm and 13.9 nm, *Nat. Photonics* **2**, 94 (2008).
- [23] Y. Kobayashi, O. Yoshihara, Y. Nabekawa, K. Kondo, and S. Watanabe, Femtosecond measurement of high-order harmonic pulse width and electron recombination time by field ionization, *Opt. Lett.* **21**, 417 (1996).
- [24] Y. Kobayashi, T. Sekikawa, Y. Nabekawa, and S. Watanabe, 27-fs extreme ultraviolet pulse generation by high-order harmonics, *Opt. Lett.* **23**, 64 (1998).
- [25] T. Sekikawa, T. Katsura, S. Miura, and S. Watanabe, Measurement of the Intensity-Dependent Atomic Dipole Phase of a High Harmonic by Frequency-Resolved Optical Gating, *Phys. Rev. Lett.* **88**, 193902 (2002).
- [26] J. M. Schins, P. Breger, P. Agostini, R. C. Constantinescu, H. G. Muller, G. Grillon, A. Antonetti, and A. Mysyrowicz, Observation of Laser-Assisted Auger Decay in Argon, *Phys. Rev. Lett.* **73**, 2180 (1994).
- [27] A. Bouhal, R. Evans, G. Grillon, A. Mysyrowicz, P. Breger, P. Agostini, R. C. Constantinescu, H. G. Muller, and D. von der Linde, Cross-correlation measurement of femtosecond non-

- collinear high-order harmonics, *J. Opt. Soc. Am. B* **14**, 950 (1997).
- [28] M. Hentschel, R. Kienberger, C. Spielmann, G. A. Reider, N. Milosevic, T. Brabec, P. Corkum, U. Heinzmann, M. Drescher, and F. Krausz, Attosecond metrology, *Nature (London)* **414**, 509 (2001).
- [29] K. Oguri, H. Nakano, T. Nishikawa, and N. Uesugi, Cross-correlation measurement of ultrashort soft X-ray pulse emitted from femtosecond laser-produced plasma using optical field-induced ionization, *Appl. Phys. Lett.* **79**, 4506 (2001).
- [30] K. Oguri, T. Ozaki, T. Nishikawa, and H. Nakano, Femtosecond-resolution measurement of soft X-ray pulse duration using ultra-fast population increase of singly charged ions induced by optical-field ionization, *Applied Physics B: Lasers and Optics* **78**, 157 (2004).
- [31] K. Oguri, T. Nishikawa, T. Ozaki, and H. Nakano, Sampling measurement of soft X-ray-pulse shapes by femtosecond sequential ionization of Kr<sup>+</sup> in an intense laser field, *Opt. Lett.* **29**, 1279 (2004).
- [32] O. Krupin, M. Trigo, W. F. Schlotter, M. Beye, F. Sorgenfrei, J. J. Turner, D. A. Reis, N. Gerken, S. Lee, W. S. Lee, G. Hays, Y. Acremann, B. Abbey, R. Coffee, M. Messerschmidt, S. P. Hau-Riege, G. Lapertot, J. Lüning, P. Heimann, R. Soufli *et al.*, Temporal cross-correlation of X-ray free electron and optical lasers using soft X-ray pulse induced transient reflectivity, *Opt. Express* **20**, 11396 (2012).
- [33] U. Teubner, U. Wagner, and E. Förster, Sub-10 fs gating of optical pulses, *J. Phys. B: At. Mol. Opt. Phys.* **34**, 2993 (2001).
- [34] R. Keenan, J. Dunn, P. K. Patel, D. F. Price, R. F. Smith, and V. N. Shlyaptsev, High-Repetition-Rate Grazing-Incidence Pumped X-Ray Laser Operating at 18.9 nm, *Phys. Rev. Lett.* **94**, 103901 (2005).
- [35] M. Grünig, C. Imesch, F. Staub, and J. Balmer, Saturated X-ray lasing in Ni-like Sn at 11.9 nm using the GRIP scheme, *Optics Communication* **282**, 267 (2009).
- [36] S. Handa, T. Kimura, H. Mimura, H. Yumoto, S. Matsuyama, Y. Sano, K. Tamasaku, Y. Nishino, M. Yabashi, T. Ishikawa, and K. Yamauchi, Extended knife-edge method for characterizing sub-10-nm X-ray beams, *Nucl. Instrum. Methods Phys. Res. Sect. A* **616**, 246 (2009).
- [37] F. Tissandier, S. Sebban, M. Ribiere, J. Gautier, P. Zeitoun, G. Lambert, A. B. Sardinha, J.-P. Goddet, F. Burgy, T. Lefrou, C. Valentin, A. Rouse, O. Guilbaud, A. Klisnick, J. Nejd, T. Mocek, and G. Maynard, Observation of spectral gain narrowing in a high-order harmonic seeded soft X-ray amplifier, *Phys. Rev. A* **81**, 063833 (2010).
- [38] E. Oliva, M. Cotelo, J. C. Escudero, A. González-Fernández, A. Sanchís, J. Vera, S. Vicéns, and P. Velarde, DAGON: a 3D Maxwell-Bloch code, *Proc. SPIE 10243, X-ray Lasers and Coherent X-ray Sources: Development and Applications*, Vol. 10243 (SPIE, USA, 2017).
- [39] E. Oliva, E. V. Fernandez-Tello, M. Cotelo, P. M. Gil, J. A. Moreno, and P. Velarde, 3D multi-scale modelling of plasma-based seeded soft X-ray lasers, *The European Physical Journal D* **75**, 290 (2021).
- [40] F. Ogando and P. Velarde, Development of a radiation transport fluid dynamic code under AMR scheme, *Journal of Quantitative Spectroscopy & Radiative Transfer* **71**, 541 (2001).
- [41] M. Cotelo, P. Velarde, A. de la Varga, D. Portillo, C. Stehlé, U. Chaulagain, M. Kozlova, J. Larour, and F. Suzuki-Vidal, Simulation of radiative shock wave in Xe of last PALS experiments, *High Energy Density Phys.* **17**, 68 (2015), 10th International Conference on High Energy Density Laboratory Astrophysics.
- [42] R. Lehe, M. Kirchen, I. A. Andriyash, B. B. Godfrey, and J.-L. Vay, A spectral, quasi-cylindrical and dispersion-free particle-in-cell algorithm, *Comput. Phys. Commun.* **203**, 66 (2016).
- [43] B. Cros, T. Mocek, I. Bettaibi, G. Vieux, M. Farinet, J. Dubau, S. Sebban, and G. Maynard, Characterization of the collisionally pumped optical-field-ionized soft X-ray laser at 41.8nm driven in capillary tubes, *Phys. Rev. A* **73**, 033801 (2006).
- [44] F. Tuitje, P. M. Gil, T. Helk, J. Gautier, F. Tissandier, J.-P. Goddet, A. Guggenmos, U. Kleineberg, S. Sebban, E. Oliva, C. Spielmann, and M. Zürch, Nonlinear ionization dynamics of hot dense plasma observed in a laser-plasma amplifier, *Light Sci. Appl.* **9**, 187 (2020).